

# Alterations in the Transcriptional Programs of Myeloma Cells and the Microenvironment during Extramedullary Progression Affect Proliferation and Immune Evasion

Daeun Ryu<sup>1,2,3</sup>, Seok Jin Kim<sup>4</sup>, Yourae Hong<sup>1</sup>, Areum Jo<sup>1,2,3</sup>, Nayoung Kim<sup>1,2,3</sup>, Hee-Jin Kim<sup>5</sup>, Hae-Ock Lee<sup>1,2,3</sup>, Kihyun Kim<sup>4</sup>, and Woong-Yang Park<sup>1,2,3</sup>



## ABSTRACT

**Purpose:** In multiple myeloma, extramedullary progression is associated with treatment resistance and a high mortality rate. To understand the molecular mechanisms controlling the devastating progression of myeloma, we applied single-cell RNA-sequencing (RNA-seq) to myeloma in the bone marrow and myelomatous pleural effusions or ascites.

**Experimental Design:** Bone marrow or extramedullary myeloma samples were collected from 15 patients and subjected to single-cell RNA-seq. The single-cell transcriptome data of malignant plasma cells and the surrounding immune microenvironment were analyzed.

**Results:** Comparisons of single-cell transcriptomes revealed the systematic activation of proliferation, antigen presentation, proteasomes, glycolysis, and oxidative phosphorylation pathways in extramedullary myeloma cells. The myeloma cells expressed

multiple combinations of growth factors and receptors, suggesting autonomous and pleiotropic growth potential at the single-cell level. Comparisons of the tumor microenvironment revealed the presence of cytotoxic T lymphocytes and natural killer (NK) cells in both the bone marrow and extramedullary ascites, demonstrating a gene-expression phenotype indicative of functional compromise. In parallel, isolated myeloma cells persistently expressed class I MHC molecules and upregulated inhibitory molecules for cytotoxic T and NK cells.

**Conclusions:** These data suggest that myeloma cells are equipped with specialized immune evasion mechanisms in cytotoxic microenvironments. Taken together, single-cell transcriptome analysis revealed transcriptional programs associated with aggressive myeloma progression that support autonomous cell proliferation and immune evasion.

## Introduction

Multiple myeloma, a plasma cell malignancy in the bone marrow, begins as a monoclonal gammopathy of undetermined significance (MGUS) and eventually progresses to extramedullary disease (1). Extramedullary myeloma commonly affects the pleura, lymph nodes, soft tissues, and liver and is an aggressive disease associated with treatment resistance and shorter patient survival times (2). Early extramedullary or ascites involvement at diagnosis is rare and particularly detrimental.

Cytogenetic and genetic analyses have been performed to identify the molecular characteristics associated with aggressive extramedullary myeloma progression. Cytogenetic abnormalities involving t(4;14) or t(14;16) translocations are early genetic events with poor prognosis, whereas the 17p deletion, which is the most significant genetic prognostic factor in multiple myeloma, occurs during disease progression (3). In addition, *MYC* translocations and mutations in *TP53*, *CCND1*, *ATM*, *ATR*, and *ZFHX4* have a negative prognostic impact (3). Extramedullary myeloma has a higher incidence of the t(4;14) translocation, 17p deletion, and *MYC* overexpression and often manifests with different cytogenetics than matched bone marrow myeloma (4), indicating genomic instability. Gene-expression profiling-based risk stratification using many proliferation genes classifies patients with extramedullary myeloma as a high-risk group (5).

The cytogenetic, genetic, and gene-expression profiles of extramedullary myeloma are enriched for poor prognostic alterations, suggesting an intrinsically aggressive nature. As extramedullary myeloma progression requires bone marrow-independent growth and survival, it must gain an alternative source of growth/survival signals and immune suppression signals that would normally be provided by the bone marrow niche (6). The inextricable relationship between myeloma and its microenvironment requires the characterization of both components to understand the progression of myeloma to non-bone marrow compartments.

In this study, we used single-cell RNA sequencing (RNA-seq) to carry out the genomic characterization of diverse cell populations without experimental separation (7). We combined two single-cell RNA (scRNA)-sequencing approaches, high-throughput RNA-seq for the simultaneous analysis of myeloma, and the immune microenvironment and full-length RNA-seq of purified myeloma cells for molecular pathway analyses. We show that extramedullary

<sup>1</sup>Samsung Genome Institute, Samsung Medical Center, Seoul, Korea. <sup>2</sup>Department of Health Sciences and Technology, Samsung Advanced Institute for Health Sciences and Technology, Sungkyunkwan University School of Medicine, Seoul, Korea. <sup>3</sup>Department of Molecular Cell Biology, Sungkyunkwan University School of Medicine, Seoul, Korea. <sup>4</sup>Division of Hematology-Oncology, Department of Medicine, Samsung Medical Center, Sungkyunkwan University School of Medicine, Seoul, Korea. <sup>5</sup>Department of Laboratory Medicine and Genetics, Sungkyunkwan University School of Medicine, Seoul, Korea.

**Note:** Supplementary data for this article are available at Clinical Cancer Research Online (<http://clincancerres.aacrjournals.org/>).

Corrected online 9/1/2020.

**Corresponding Authors:** Woong-Yang Park, Samsung Medical Center, 81 Irwonro, Gangnamgu, Seoul 06351, Korea. Phone: 822-2148-9810; Fax: 822-2148-9819; E-mail: woonyang@skku.edu; Hae-Ock Lee, Samsung Genome Institute, Samsung Medical Center, Seoul, Korea. E-mail: haeock.lee@samsung.com; and Kihyun Kim, Division of Hematology-Oncology, Department of Medicine, Samsung Medical Center, Sungkyunkwan University School of Medicine, Seoul, Korea. E-mail: kihyunk.kim@samsung.com

Clin Cancer Res 2020;26:935-44

doi: 10.1158/1078-0432.CCR-19-0694

©2019 American Association for Cancer Research.

### Translational Relevance

Single-cell RNA sequencing reveals the myeloma transcriptome landscape in the context of the immune microenvironment.

Extramedullary myeloma progression is associated with heterogeneous mechanisms of growth factor stimulation and immune evasion.

myeloma cells exhibit autonomous and multiple growth factor-receptor expression that can drive massive cell proliferation in a bone marrow-independent manner. Second, extramedullary myeloma cells possess heterogeneous immune evasion mechanisms against NK and cytotoxic T cells accompanied by the functional impairment of immune cells. By analyzing the myeloma transcriptome aligned with tumor progression, we identified transcriptional programs controlling the progression of aggressive extramedullary myeloma.

## Materials and Methods

### Patients and sample preparation

This study was approved by the Institutional Review Board (IRB) of Samsung Medical Center (IRB approval no. SMC2013-09-009-012) and carried out in accordance with the principles of the Declaration of Helsinki. Informed written consent was obtained from each subject. The study subjects were 15 Korean patients diagnosed with multiple myeloma at the Samsung Medical Center (Seoul, Korea). Four bone marrow aspirates, one ascites, and two pleural effusion samples were subjected to red blood cell lysis (Qiagen) and cryopreserved in CELLBANK1 (Zenoaq) before 3' scRNA sequencing. Nine bone marrow aspirate samples were subjected to a Ficoll-Paque PLUS (GE Healthcare) gradient and magnetic separation with anti-CD138 antibody microbeads (Miltenyi Biotec). Ascites (2 patients) and pleural effusion (1 patient) samples were collected and subjected to the same cell isolation process. CD138-positive myeloma-enriched fractions were immediately used for full-length scRNA sequencing, except for one sample (MM26 ascites) that was cryopreserved. Genomic DNA and RNA were purified from CD138-positive and CD138-negative fractions using an ALLPrep kit (Qiagen). Corresponding blood DNA was isolated using a QIAamp DNA Blood Kit (Qiagen).

### Exome sequencing and data processing

Genomic DNA from the bone marrow and corresponding blood samples was sheared by Covaris S220 (Covaris) and libraries were constructed using a SureSelect XT Human All Exon v5 and a SureSelect XT Reagent Kit, HSQ (Agilent Technologies) according to the manufacturer's protocol. After multiplexing, the libraries were sequenced on a HiSeq 2500 sequencing platform (Illumina) using the 100 bp paired-end mode of the TruSeq Rapid PE Cluster Kit and TruSeq Rapid SBS Kit (Illumina).

Sequencing reads were aligned to the UCSC hg19 reference genome (<http://genome.ucsc.edu>) using Burrows-Wheeler Aligner version 0.6.2 with the default options. PCR duplications and data cleanup were marked using Picard-tools-1.8 (<http://picard.sourceforge.net/>) and GATK-2.2.9 (<https://www.broadinstitute.org/gatk/>). Single-nucleotide variants of paired samples were identified by MuTect (<https://github.com/broadinstitute/mutect>) and annotated using ANNOVAR.

### RNA-seq and data processing

Whole-transcriptome sequencing libraries were generated for the RNAs from CD138-negative cell fractions using a TruSeq RNA Sample Preparation v2 Kit (Illumina). Sequencing was carried out using the 100 bp paired-end mode of the TruSeq Rapid PE Cluster Kit and TruSeq Rapid SBS Kit (Illumina).

For full-length scRNA sequencing, CD138-positive myeloma cells were loaded onto a 5 to 10  $\mu$ m integrated fluidic circuit mRNA sequencing chip for microscopic examination, lysis, reverse transcription, and cDNA amplification in the C1 Single-Cell Auto Prep System (Fluidigm), according to the manufacturer's instructions. RNA spike-ins 1, 4, and 7 from ArrayControl RNA spikes (Thermo Fisher Scientific) were added to the lysis solution according to the manufacturer's instructions. For MM02EM, 96 External RNA Controls Consortium spike-in sequences (Thermo Fisher Scientific) were used instead. Sequencing libraries were constructed using amplified cDNAs with the Nextera XT DNA Sample Prep Kit (Illumina) and sequenced using the 100 bp paired-end mode of the TruSeq Rapid PE Cluster kit and TruSeq Rapid SBS Kit (Illumina). Reads from bulk and C1 RNA-seq (single cells and whole transcriptome) were mapped on to the GRCh37.75 human reference genome using STAR (<https://github.com/alexdobin/STAR/releases>) version 2.4.0 and transcripts were quantified as transcript per million (TPM) using RSEM version 1.2.18 (<http://deweylab.biostat.wisc.edu/rsem/>).

For 3' scRNA sequencing, each single-cell suspension was loaded into a GemCode system version 2 (10X Genomics) targeting 5,000 cells. Sequencing libraries were generated and sequenced on a HiSeq 2500 (Illumina) using the 100 bp paired-end mode. Sequencing reads were mapped on to the GRCh38 human reference genome using the Cell Ranger toolkit (version 2.1.0). scRNA sequencing data for normal bone marrow were downloaded from the HCA Data Portal (<https://preview.data.humancellatlas.org/>). Before downstream analyses, we applied three quality measures of mitochondrial gene percentages (<20%), unique molecular identifiers (UMI, over 1,000), and gene counts (over 20) calculated from the raw gene-cell-barcode matrix.

### Single-cell transcriptome analysis

For the 3' scRNA sequencing data, UMI counts were normalized to TPM-like values and used in the scale of  $\log_2$  (TPM+1), as described previously (8). Variable genes were selected using the R package Seurat R toolkit (ref. 9; <https://satijalab.org/seurat/>) and used to compute principal components (PC). Significant PCs were used for cell clustering and t-distributed stochastic neighbor embedding (tSNE) visualization. Before malignant plasma cell (MPC) clustering, the *Regress-Out* function was applied to remove the sample-specific batch effect. Before immune cell clustering, immunoglobulin genes were excluded from the analysis. Differentially expressed genes (DEG) were selected for each cell cluster using the Seurat package with default parameters and Student t tests. Immune cell identity annotations were defined for each cluster by reference-based single-cell annotations in the R package SingleR (<https://github.com/dviraran/SingleR>; ref. 10). Because SingleR calculates the correlation to the reference transcriptome for each cell, clusters were annotated using the dominant cell type within the cluster.

For the full-length scRNA sequencing data, reference sequences were modified by merging with external spike-in sequences (Thermo Fisher Scientific). Gene quantification data were filtered by eliminating zero-expressed genes and applying the following criteria: (i) in genes, the number of zeros should be less than 449 (mean zero count) across all samples, and (ii) in cells, the number of genes expressed in each sample should be over 1,000. To visualize the myeloma

transcriptomic landscape, tSNE and k-means clustering was performed using 11,664 genes and curated gene sets in the molecular signature database (v6.0 MSigDB). To analyze pathway activation, we performed gene set variation analysis (GSVA; ref. 11) and gene set enrichment analysis (GSEA; ref. 12) using hallmark, curated (chemical and genetic perturbations, CGP), and gene ontology gene sets in the MSigDB. For trajectory analysis, monocle 2 (13) was utilized with the default parameters.

### Flow cytometry

Peripheral blood was obtained from 5 healthy donors (average age 60.6) and 10 newly diagnosed myeloma patients (average age 64.8) within the IRB protocol SMC2013-09-009-012. Informed written consent was obtained from each subject. After red blood cell lysis (Qiagen), the whole-cell pellet was cryopreserved in CELLBANK1, rapidly thawed, and stained with PerCP-anti-CD3 (clone UCHT1), PE/Cy7-anti-CD56 (clone 5.1H11), and Alexa647-anti-GZMB (clone GB11) mAbs (BioLegend) according to the manufacturer's protocol. Flow cytometry data were obtained by FACVerse and analyzed by FlowJo software (BD Biosciences).

## Results

### Single-cell transcriptome landscape of multiple myeloma

To understand the cellular dynamics associated with myeloma progression, we first applied massively parallel single-cell RNA-seq (7) to myeloma-stricken bone marrow or extramedullary sites (Fig. 1 and Table 1). The aggregated transcriptome analysis of seven myeloma samples (four bone marrow, one ascites, and two pleural effusion) revealed patient-specific clusters of MPCs and diverse immune cell clusters shared by patients (Fig. 2A and B). The immune cell clusters were mainly comprised of mature T-cell types, NK cells, and monocytes/macrophages, as well as small numbers of B-cell-lineage cells, erythroid cells, and granulocytes (Fig. 2B; Supplementary Fig. S1A; Supplementary Table S1). Myelomatous pleural effusion and ascites samples contained a large number of MPCs and relatively few immune cells likely due to the microenvironment and highly advanced disease state (Fig. 2C, left).

The major immune cell types in the myelomatous bone marrow were similar to those in the healthy bone marrow (7, 14) but contained fewer B-cell populations (B cells and progenitors), indicating deregulated B-cell development (Fig. 2C, right; Supplementary Fig. S1B; ref. 15). Within the T and NK cell types, more CD4<sup>+</sup> naive T-cell populations were recovered from the healthy bone marrow, whereas the myeloma bone marrow was populated with more cytotoxic CD8<sup>+</sup> T cells and NK cells (Fig. 2C, right). To determine whether the expansion of cytotoxic immune cell populations could be systemically detected, we assessed GZMB (granzyme B) expression on the peripheral blood cells (Supplementary Fig. S2). The number of GZMB<sup>+</sup> T cells or NK cells in the patients with myeloma was highly variable, with CD8<sup>+</sup> T cells and NK cells from both healthy and myelomatous bone marrow also expressing variable levels of cytotoxic mediator genes (Fig. 2D, top). Moreover, regulatory and exhaustion gene expression (16) was slightly elevated in the patients with myeloma (Fig. 2D, middle), tipping the balance between exhaustion and cytotoxicity toward an exhausted state (Fig. 2D, bottom). These data suggest the activation and persistence of cytotoxic T and NK cells in the patients with myeloma, likely undergoing exhaustion.

The *in silico* separation of MPCs and subsequent clustering revealed that myeloma subpopulations (Fig. 2E) demonstrated many gene-

expression traits implicated in myeloma progression (Supplementary Table S2). The majority of bone marrow myeloma cells shared transcriptome features forming multipatient clusters (Fig. 2E; clusters 0, 7, 12). These bone marrow myeloma-enriched clusters expressed AP-1 (Fig. 2F; cluster 0; *JUN*, *FOS*; ref. 17) or *TNFRSF17* (clusters 7, 12; ref. 18), genes that promote myeloma growth and survival in the bone marrow microenvironment. In contrast, primary refractory (MM173BM) or extramedullary (MM173EM, MM26EM, and MM36EM) myeloma cells formed patient-specific clusters with heightened intratumoral heterogeneity (Fig. 2E, right and bottom). The clustering results partially reflected the expression patterns of myeloma driver genes (Supplementary Fig. S3A). MM36EM ascites myeloma contained subpopulations with proliferative and poor prognostic (Fig. 2F; cluster 6; *CKS1B*; ref. 19) gene expression, as well as inflammatory and angiogenic (cluster 1; *CCL3* and *TMSB4X*; refs. 20, 21), immune suppressive (cluster 5; *TNFSF10*; ref. 22), or potentially dexamethasone resistant (cluster 11; *NEATI*; ref. 23) marker genes (Fig. 2F; Supplementary Table S2). MM173BM and MM173EM myelomas shared *MYBL2*<sup>hi</sup> subpopulations (Fig. 2F; clusters 2, 8, 10) with proliferative (cluster 10; *UBE2S*; ref. 19) or metabolic (cluster 8; *PKM*; ref. 24) gene expression, while the MM173 metabolic subpopulation exclusively emerged during extramedullary progression (Supplementary Fig. S3B). MM26EM effusion myeloma contained *WFDC2*<sup>+</sup> (cluster 3) subpopulations recently identified by single-cell RNA-seq (25) and additional *ADM*<sup>+</sup> (cluster 4) hypoxia-induced subpopulations (26). We suspect that the number of myeloma subpopulations and their transcriptional states likely differ for individual patients and their disease status. Nonetheless, intratumoral heterogeneity suggests that myeloma survival and progression is a collaborative process between heterogeneous myeloma subpopulations that drive cancer cell proliferation, migration, immune evasion, and/or drug resistance.

### Molecular pathway activation in aggressive extramedullary myeloma cells

To understand the molecular pathways activated during the progression of aggressive myeloma, we focused on the single-cell transcriptome analysis of CD138-purified myeloma cells (Fig. 1 and Table 1). We obtained bone marrow biopsies from nine patients with stable or primary refractory disease and extramedullary samples of pleural effusion or ascites from four patients. Bone marrow and extramedullary samples were serially collected from two patients. Single-cell transcriptome data were generated using the C1 Single-Cell AutoPrep System, which allowed full-length RNA-seq with a higher coverage of lowly expressed genes than 10X system (Supplementary Fig. S4A). The mutational landscape of our patient cohort was determined by whole-exome sequencing, which identified *KRAS* and *NRAS* mutations as the most frequent genetic aberrations (Table 1). Many patients carried oncogenic translocations such as t(4;14) IgH-WHSC1, t(11;14) IgH-CCND1, or t(14;20) IgH-MAFB fusions. Thus, most patients had well-characterized genetic aberrations frequently found in multiple myeloma (27).

Following data quality filtration, we acquired full-length RNA-seq data from 492 cells, with an average of 4.7 million sequencing reads and 4,924 genes in each myeloma cell. Externally spiked-in RNA sequences (Supplementary Fig. S4B) show a constant level of detection across all cells and patients, ensuring high-quality single-cell sequencing with a low batch effect. Individual myeloma cells expressed clonotypic immunoglobulin sequences within a single patient (Supplementary Fig. S4C left; ref. 28) and plasma cell-specific transcription factors (*PRDM1*, *IRF4*, and *XBPI*) with a lack of mature B cells (*PAX5* and

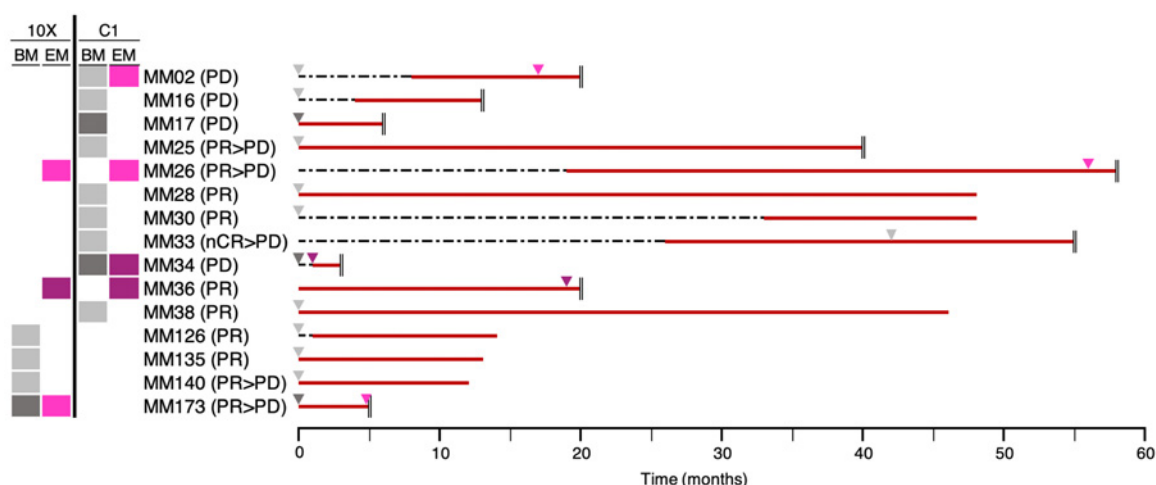


**Figure 1.**

Myeloma sample configuration for single-cell RNA-seq. Myeloma samples from 15 patients were collected from the bone marrow (gray) or extramedullary sites (magenta) and subjected to single-cell RNA-seq using the 10X or C1 platform (pale gray: bone marrow; dark gray: primary refractory bone marrow; pale magenta: pleural effusion; dark magenta: ascites). All 10X data were generated from cryopreserved samples, whereas fresh samples were used for C1 data (except for MM26EM, cryopreserved). On the right, sampling time points (arrows) at initial diagnosis or during disease progression. Periods of bortezomib treatment (red lines) and the treatment response (parentheses) are indicated. Black dotted lines mark pretreatment and red solid lines mark bortezomib posttreatment periods. Patient death is marked as "||." BM, bone marrow with survival periods over 6 months; primary refractory BM (PRBM), with survival periods under 6 months (MM17, MM34, and MM173); EM, extramedullary (MM02, MM26, MM34, MM36, and MM173); nCR, near complete response; PD, progressive disease; PR, partial response.

*BACH2*; Supplementary Fig. S4C, right; ref. 29). Transcripts for plasma cell-surface molecules, such as *SDC1* (*CD138*), *CD38*, and *SLAMF7*, were consistently expressed in most myeloma cells and are candidate therapeutic targets for multiple myeloma (30).

Using the full-length single-cell transcriptome data, we performed clustering analysis on all the bone marrow and extramedullary myeloma cells from 11 patients (Fig. 3A). We eliminated immunoglobulin genes from the clustering analysis as their high

**Table 1.** Clinical and genomic characteristics for the patients with myeloma.

Patients	Sex	Age	ISS	Survival time (months)	Heavy chain	Light chain	Cytogenetics	FISH	Mutations
MM02	M	50	II	20(3) <sup>a</sup>	IgG	κ	N	tri1q	KRAS(NM_004985:p.G13C)
MM16	F	31	II	13	IgG	κ	NH	del13, del17p13	KRAS(NM_004985:p.G13D), TP53(NM_000546:p.L344R,p.R110L), NFKB2(NM_002502:p.H639P)
MM17	F	65	II	6	IgG	κ	NH	tri1q, t(4;14)	
MM25	M	74	-	40	-	λ	NH	tri1q, del17p13, t(11;14)	NRAS(NM_002524:p.Q61K), CCND1(NM_053056:p.Y44C,p.K114R,p.E122D)
MM26	F	51	III	58(1) <sup>a</sup>	IgG	κ	N	t(4;14)	
MM28	M	77	II	41 <sup>b</sup>	-	κ	N		NRAS(NM_002524:p.G13R)
MM30	F	62	II	41 <sup>b</sup>	IgG	κ	HD	tri1q	NRAS(NM_002524:p.Q61H)
MM33	F	50	III	55	-	λ	NH		
MM34	F	42	III	3(1) <sup>a</sup>	IgG	κ	NH	tri1q, del13, del17p13, t(14;20)	
MM36	M	57	I	20(1) <sup>a</sup>	IgG	λ	NH	tri1q, del13, t(4;14)	BRAF(NM_004333:p.V600E), MYO10(NM_012334:p.R147C)
MM38	F	66	I	39 <sup>b</sup>	IgG	κ	HD		NRAS(NM_002524:p.Q61K)
MM126	M	64	II	14 <sup>b</sup>	IgG	λ	HD	del13	MYO10(NM_012334:p.E973K)
MM135	F	58	II	13 <sup>b</sup>	IgA	λ	NH	del13, del17p13, t(4;14)	
MM140	M	56	II	12 <sup>b</sup>	IgG	λ	N		
MM173	M	64	III	5(0) <sup>a</sup>	IgD	λ	NH		KRAS(NM_004985:p.Q61H)

Note: Parentheses indicate survival time from EM sampling to death.

Abbreviations: EM, extramedullary; HD, hyperdiploid; N, normal; NH, nonhyperdiploid.

<sup>a</sup>Patients with EM sampling.

<sup>b</sup>Patients alive at the most recent follow-up. For survival time: from the date of diagnosis to death or follow-up periods for b.

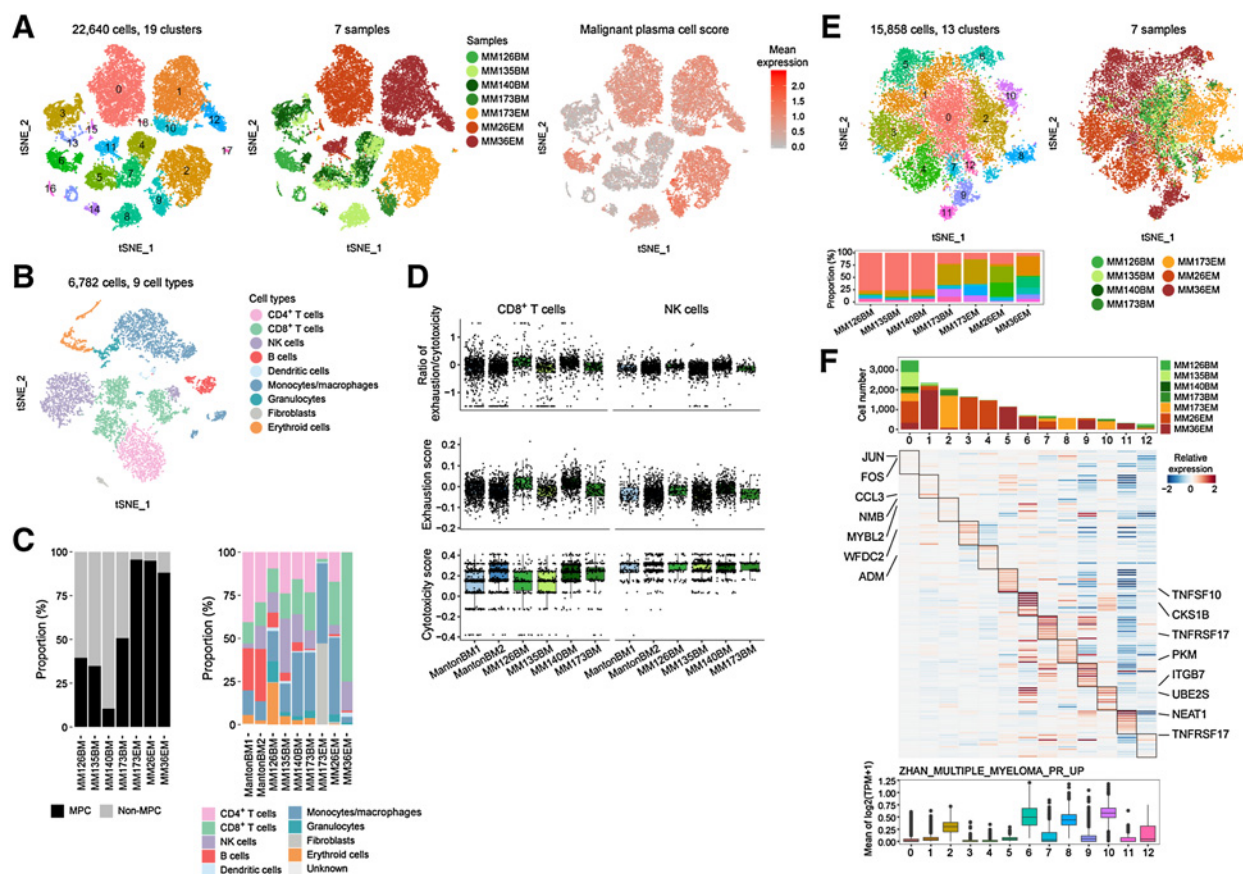


**Figure 2.**

Transcriptome landscape of multiple myeloma drawn from 3' scRNA sequencing. The 3' scRNA sequencing data from seven myelomatous samples (four bone marrow, one ascites, and two pleural effusion) were aggregated and subjected to clustering using the Seurat package with the default parameters. **A**, t-SNE plots showing multiple cell-type clusters. Left, t-SNE plot of 22,640 cells color-coded by cluster. Middle, t-SNE plot color-coded by sample. Right, Plasma cell score using the average expression of 9 genes (*BACH2*, *PAX5*, *BCL6*, *PRDM1*, *IRF4*, *XBP1*, *SDC1*, *CD38*, and *SLAMF7*). **B**, t-SNE plot of 6,782 immune cells in the myeloma microenvironment, color-coded by cell type. Cell type specification was validated by SingleR. **C**, Proportion of MPCs in each sample (left). Immune cell composition of the myeloma microenvironment compared with healthy bone marrow (right). **D**, Scores for ratio of exhaustion to cytotoxicity, exhaustion, and cytotoxicity in CD8<sup>+</sup> T cells and NK cells. Scores were calculated by single-sample GSEA (ssGSEA) using gene sets provided by Tirosch and colleagues (16). **E**, t-SNE plot of 15,858 MPCs in the seven myeloma samples color-coded by cluster (left) or sample origin (right). Cluster proportions per sample are provided (bottom). **F**, Number of cells per cluster, color-coded by sample (top). Average expression map of top 10 DEGs (excluding ribosomal protein, immunoglobulin, and hemoglobin genes) for 13 clusters. The expression of each gene was centered at its average expression across all MPCs on a scale of 2 to -2 (middle). Gene-expression scores (mean expression) for multiple myeloma proliferation (MSigDB) are provided (bottom).

levels of clonotypic expression hinder the identification of other molecular pathways causing intertumoral or intratumoral heterogeneity. tSNE projection visualized extramedullary myeloma cells with distinctive patient-specific clusters, whereas most of the bone marrow cells formed common multipatient clusters (Fig. 3A). The expression of the myeloma driver genes partially contributed to the clustering results (Fig. 3B). Correlation analysis at the gene expression (Fig. 3C, left) or pathway level (right) substantiated the overall separation of the extramedullary myeloma cells from the bone marrow myeloma cells. At the pathway level, the primary refractory bone marrow myeloma cells (MM17 and MM34) resembled those of the extramedullary myeloma cells. To extract features of aggressive extramedullary myeloma progression, we made pair-wise comparisons between the bone marrow and extramedullary myeloma cells (Fig. 3D and Supplementary Table S3). We identified transcriptional changes in the upregulation

of proliferation/cell-cycle progression, glycolysis, oxidative phosphorylation, proteasome, and antigen presentation genes upon aggressive extramedullary myeloma progression, while bone marrow myeloma cells expressed higher levels of “TNF $\alpha$ -induced NF- $\kappa$ B pathway” genes. All pathways have also been identified by other single-cell analysis methods (Supplementary Fig. S4D; ref. 31). Intriguingly, we found gradual unidirectional changes in most pathway signatures of bone marrow cells from stable disease toward primary refractory and extramedullary progression (Fig. 3E). The NF- $\kappa$ B pathway was the exception, being upregulated in primary refractory bone marrow cells but downregulated in most extramedullary cells. Complex regulation of the NF- $\kappa$ B pathway was observed from correlation analysis between the pathways (Fig. 3F), suggesting that the NF- $\kappa$ B pathway plays a differential role in myeloma progression within the bone marrow or extramedullary microenvironment.



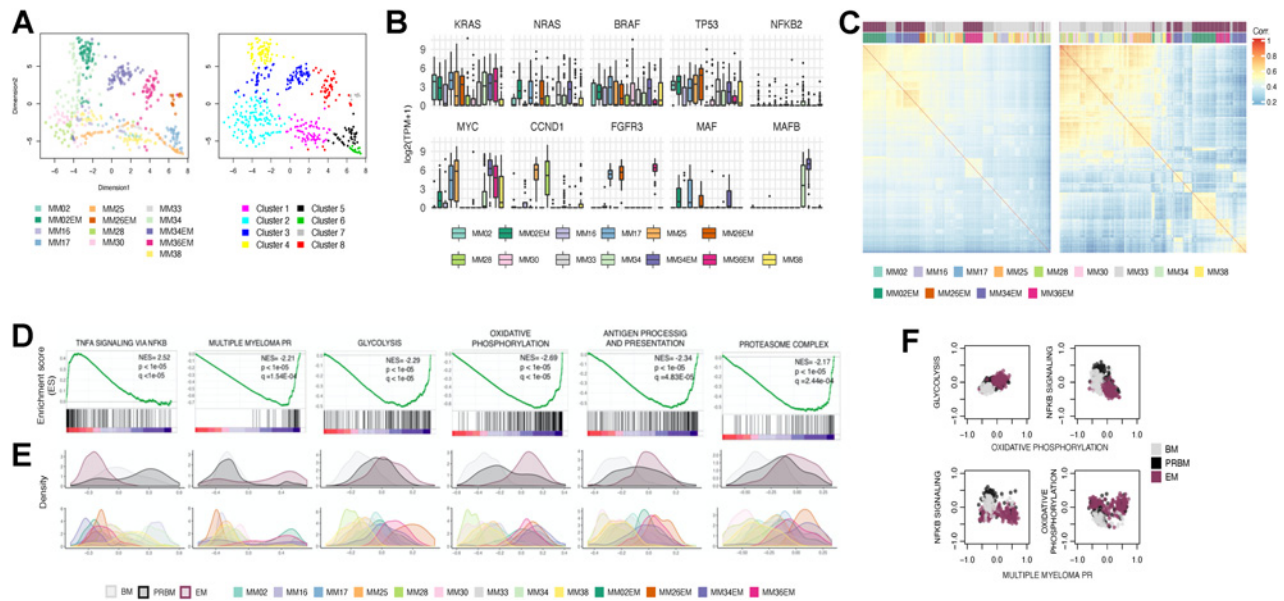


**Figure 3.** Molecular pathway activation associated with extramedullary progression. Transcriptomic changes during aggressive myeloma progression were analyzed from the full-length scRNA sequencing data of purified myeloma cells. **A**, tSNE plots, colored by sample and cluster (k-means clustering, k = 8). **B**, Gene expression associated with genetic aberrations in the myeloma patients. **C**, Clustering by Pearson correlation between cells using gene expression (left) or CGP pathways (right). **D**, Selected GSEA results between myeloma cells in the bone marrow (BM) versus extramedullary (EM) sites. **E**, Density plots showing changes in GSEA scores for the BM, primary refractory bone marrow (PRBM), and EM groups (top) or by patient (bottom). **F**, Scatter plots of GSEA demonstrate relationships between glycolysis, oxidative phosphorylation, proliferation, and NF- $\kappa$ B signaling activation.

**Effect of single-cell transcriptome signatures on patient survival**

To assess the importance of five gene-expression signatures (proliferation, glycolysis, oxidative phosphorylation, antigen processing and presentation, and proteasome) selected from the single-cell transcriptome data, we determined their impacts on patient survival using two cohorts with extensive clinical annotation: GSE24080 (32) and GSE9782 (33). In the newly diagnosed multiple myeloma GSE24080 cohort, the proliferation signature had poor prognostic value for overall survival (Fig. 4A; Supplementary Table S4A), while in the relapsed multiple myeloma GSE9782 cohort, antigen presentation, proteasome, glycolysis, and oxidative phosphorylation signatures predicted poor prognosis (Fig. 4B; Supplementary Table S4B). The

proliferation signature had less of an impact on overall survival in relapsed myeloma, suggesting that increased proliferation is involved in primary relapse, whereas upregulated antigen presentation, proteasome, glycolysis, and oxidative phosphorylation have a more profound effect on the later aggressive progression and/or treatment resistance of relapsed myeloma.

**Mechanisms driving massive myeloma proliferation**

To elucidate the mechanisms driving massive proliferation in aggressive extramedullary myeloma cells, we examined the expression levels of myeloma growth and survival factors. Of the 148 genes known to affect myeloma cell growth (6, 34), we detected 32 genes expressed by the myeloma cells (Fig. 5A). Most of the growth factors, including

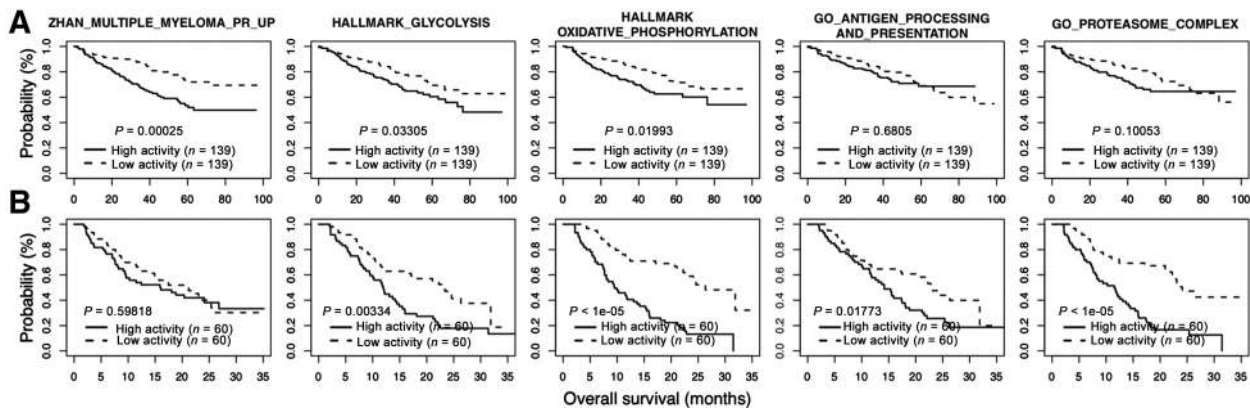


**Figure 4.** Impact of single-cell transcriptome signatures on patient survival. In univariate analyses, the associations between five gene-expression sets (multiple myeloma proliferation, glycolysis, oxidative phosphorylation, antigen processing and presentation, and proteasome complex) and overall survival were evaluated using GSE24080 (A) and GSE9782 (B) microarray data sets. Patients were grouped into upper and lower quartiles for high and low gene signature groups, respectively.

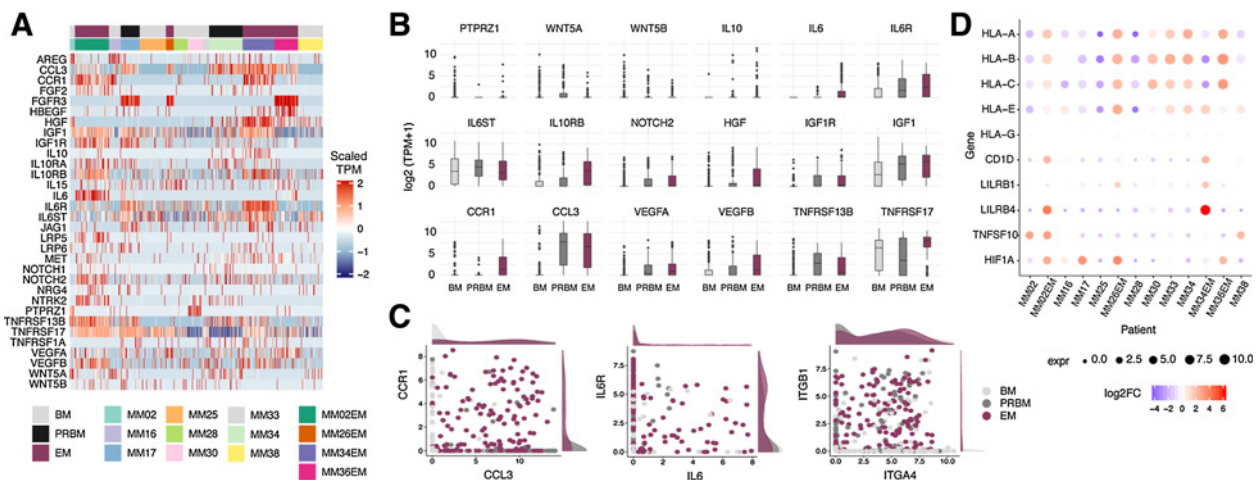


**Figure 5.**

Growth factor and immunomodulatory gene expression in extramedullary myeloma cells. **A**, Heatmap of myeloma growth factor and receptor expression; **B**, Comparisons between the bone marrow (BM), primary refractory bone marrow (PRBM), and extramedullary (EM) cells for selected myeloma growth factor/receptor gene expression. **C**, Paired growth factor receptor for  $\alpha 4\beta 1$  integrin genes in the BM, PRBM, and EM myeloma cells. Scales are  $\log_2(\text{TPM}+1)$ . **D**, NK and cytotoxic T-cell inhibitory molecular expression by myeloma cells. Circle size denotes the mean expression level in each patient. Color key represents the  $\log_2$ -fold change of each patient over the mean expression of all patients.

*CCL3* and *IL6*, were more prominently expressed in the extramedullary myeloma cells (Fig. 5B). Cognate receptor expression for these growth/survival factors may stimulate tumor growth in an autocrine or paracrine manner independently of the bone marrow microenvironment. Indeed, many extramedullary myeloma cells simultaneously expressed *CCL3* and *CCR1* or *IL6* and *IL6R*, suggesting a potential auto-/paracrine loop in the growth factor signaling axis (Fig. 5C). The expression of the *CCL3* and *IL6* genes was also assessed in the 10X data set (Supplementary Fig. S4E).

VLA4 ( $\alpha 4\beta 1$ ), formed by the *ITGA4* and *ITGB1* gene products, is the major integrin in the bone marrow and mediates myeloma cell homing and survival by interacting with the bone marrow microenvironment (35). The primary ligands of VLA4 are VCAM1 and fibronectin (*FN1* gene). We found that *ITGA4* and *ITGB1* are often coexpressed by extramedullary myeloma cells (Fig. 5C right), whereas *FN1* expression was detected in the CD138-negative nonmyeloma cell fractions of myelomatous ascites (Supplementary Fig. S4F), suggesting that myeloma growth signals are delivered to VLA4 by the extramedullary microenvironment (36). Altogether, these multiple auto- and paracrine growth signals could alleviate the dependency of myeloma growth on the bone marrow microenvironment (3, 34).

### Mechanisms of immune evasion accompanying myeloma progression

The bone marrow niche provides myeloma survival signals and an immune-suppressive microenvironment (6). Hematopoietic cells, including myeloid-derived suppressor cells and regulatory T cells, are known to be strongly involved in creating an immune-suppressive microenvironment (37). In Fig. 2, we demonstrated a significant number of cytotoxic T lymphocytes and NK cells in the myelomatous bone marrow and ascites, despite the elevated expression of exhaustion molecules. In myeloma, various mechanisms of immune evasion were detected at the gene-expression level. First, MPCs demonstrated consistent classic (*HLA-A*, *B*, and *C*) and nonclassic (*HLA-E* and *CD1D*) MHC class

I molecule expression (Fig. 5D), which could provide a mechanism of protection from NK-mediated cytotoxicity (38, 39). Sustained classic and nonclassic MHC I expression in myeloma contrasts with the frequent loss observed in other types of solid cancers (40). The expression of leukocyte immunoglobulin-like (LIL) family proteins *LILRB1* and *LILRB4* may also deliver inhibitory signals to NK cells (41, 42). Immunomodulatory gene expression by myeloma cells was also assessed in the 10X data set (Supplementary Fig. S4E), demonstrating that myeloma progression elicits multiple and heterogeneous NK-evasion pathways for tumor cells.

Overall, patients with myeloma demonstrated a shift in T-cell composition from a naïve toward a cytotoxic/exhausted phenotype, suggesting T-cell activation followed by a gradual waning (Fig. 2D). In myeloma samples, we found several gene-expression characteristics associated with evasion from cytotoxic T lymphocytes (CTL; Fig. 5D). First, MHC class I gene expression was variably regulated in the paired extramedullary samples, suggesting that myeloma cells flexibly balance MHC class I levels to avoid NK- or T-cell-mediated cytotoxicity. Second, some extramedullary myeloma cells expressed the TRAIL gene (*TNFSF10*), which may engage TRAIL receptors on T cells and trigger their aberrant activation (22). Finally transcription factor hypoxia-inducible factor-1-alpha (*HIF1A*) gene expression was upregulated in extramedullary myeloma; the exposure of cancer cells to hypoxia is known to induce the expression of programmed cell death ligand-1 (PD-L1), which increases tumor cell resistance to CTL-mediated lysis (43). Overall, these data suggest that heterogeneous mechanisms of immune evasion accompany myeloma progression.

### Intratumor heterogeneity and tumor evolution in multiple myeloma

After primary bone marrow biopsy, most patients received a combination treatment including the proteasome inhibitor bortezomib (Fig. 1). All primary refractory bone marrow myeloma (MM17, MM34, and MM173) and extramedullary samples were collected during the refractory (relapsed) phase. Multiple mechanisms can

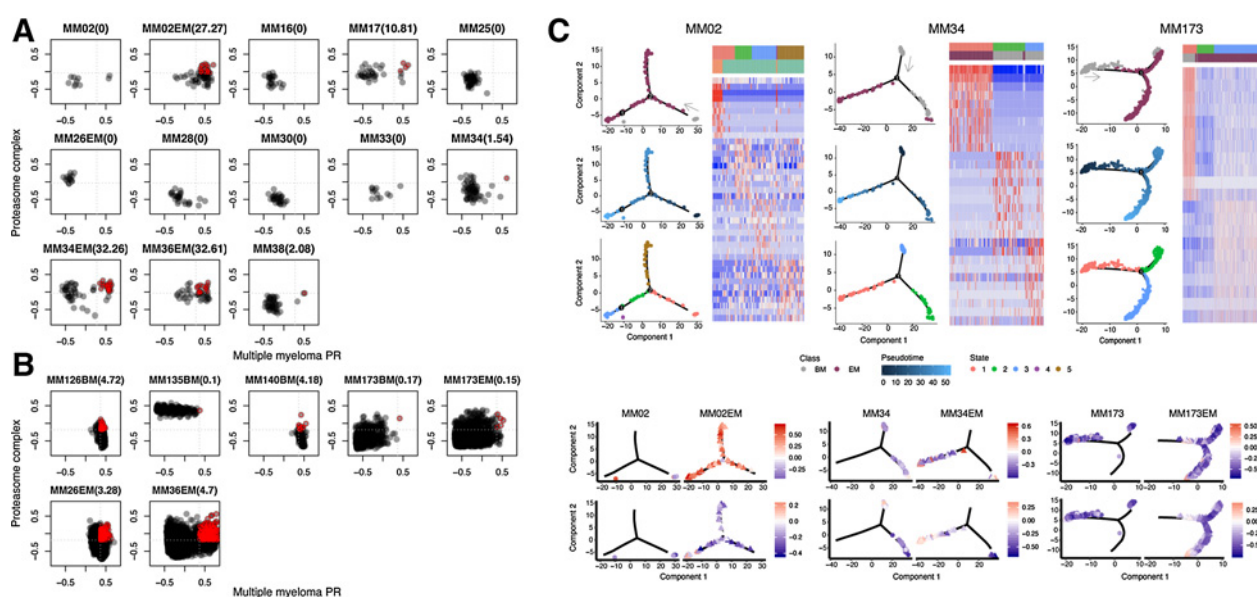


**Figure 6.**

Intratumoral heterogeneity as a potential mechanism of myeloma progression. Scatter plots of GSEA for “multiple myeloma proliferation” and “proteasome complex” are presented for myeloma cells from C1 (A) and 10X (B) platform data. Quadrants are set as the third quartile of the total GSEA score on the same platform. The proportion of myeloma cells in the top right quadrant (red circles) is indicated in parentheses next to the sample name. C, Trajectory analysis of paired samples by monocle 2 shows gene expression changes along with myeloma progression. Arrows are drawn from the bone marrow to extramedullary samples. Overlay of GSEA scores (color key) for “multiple myeloma proliferation” and “proteasome complex” shows a heterogeneous pattern between branches.

confer bortezomib resistance, among which proteasome activation occurs most frequently, involving the overexpression of proteasome components or mutations in the *PSMB5* gene (44). GSEA detected the overexpression of proteasome components in myeloma subpopulations (Fig. 3D). Some also expressed high levels of proliferation-associated genes, which is the most validated myeloma signature for poor prognosis (45). Therefore, myeloma cell subsets with both proliferation and proteasome signature expression may be highly aggressive and drug resistant (Fig. 6A and B). Single-cell analysis revealed that heterogeneity in gene expression reflects the state of myeloma subpopulations and potentially drug resistance and disease progression (46).

To examine the relationship between tumor heterogeneity and evolution in extramedullary disease, we performed a trajectory analysis for paired bone marrow–extramedullary samples, MM02(EM), MM34(EM), and MM173(EM; Fig. 6C). Both bone marrow and ascites/effusion samples from MM34 and MM173 patients were obtained during the highly aggressive refractory disease state, with an extremely short interval between the two biopsies (Fig. 1). In comparison, the MM02 bone marrow biopsy was obtained during an early disease phase and the effusion sample was collected during the relapsed refractory phase two years later. Trajectory analysis (13) of each patient revealed 3 to 5 states and visualized the evolution of the myeloma transcriptome (Fig. 6C). Pseudotime analysis indicated a branched evolution from the bone marrow to the extramedullary myeloma. Intriguingly, one of the extramedullary branches was more remotely related to bone marrow myeloma and was enriched in proliferation or proteasome gene expression compared with the others (Fig. 6C, bottom). These results suggest that intratumoral heterogeneity is linked with the evolution of more aggressive myeloma subpopulations and disease progression.

## Discussion

By combining massively parallel 3' scRNA sequencing (10X platform) and low-throughput full-length RNA-seq (C1 platform), we characterized the molecular events accompanying aggressive extramedullary myeloma progression in the context of the tumor-immune microenvironment. Massively parallel RNA-seq illustrated the overall tumor landscape encompassing the myeloma and immune microenvironment, whereas in-depth analyses of purified myeloma cells allowed the molecular characterization of individual myeloma cells. The two approaches also compensated limitations in each method, the small number of cells and cell size limitations in the C1 or extremely sparse gene expressions in the 10X platform.

Visualization of the global transcriptome landscape demonstrated the presence of diverse myeloma subpopulations surrounded by cytotoxic CD8<sup>+</sup> T cells and NK cells. In previous studies, T-cell and NK-cell defects were demonstrated in numbers, phenotypes, and function for advanced myeloma patients (47). Importantly, therapeutic strategies reversing NK or T-cell dysfunction or enhancing their activity have gained much attention and achieved clinical benefits in some cases. By comprehensive transcriptome profiling at a single-cell resolution, we demonstrated differences in T cells and NK cells, with a shift from naïve toward an activated/exhausted state. We also identified dynamic regulation of MHC class I gene expression in myeloma cells and suggested additional mechanisms of NK and T-cell inhibition, including LILRB1/4-mediated NK inhibition, TRAIL (*TNFSF10*)-mediated immune cell regulation, and HIF1A-mediated resistance from cytotoxic T-cell killing. These potential mechanisms varied among patients, suggesting differential immune cell status and the susceptibility of cytotoxic T cells and NK cells to reactivation strategies.



The most dramatic changes accompanying aggressive myeloma progression were the autocrine and pleiotropic gene-expression phenotype for myeloma growth factor receptors. In particular, the vast majority of extramedullary myeloma cells and refractory bone marrow myeloma cells expressed IL6 receptor transcripts, unlike the sparse expression among primary myeloma cells in the bone marrow (48). Many extramedullary myeloma cells simultaneously expressed *IL6*, suggesting autocrine activation and growth independence. In the bone marrow, IL6 is mainly provided from the myeloma niche by a paracrine source (34). IL6 production and downstream IL6R signaling can be amplified via other molecular interactions; for instance, the VLA4 integrin (*ITGA4* and *ITGB1* gene expression) in myeloma cells and fibronectin (*FNI* gene expression) in the CD138-negative compartment of extramedullary myeloma can augment IL6-mediated growth (49). Overall, these data demonstrate multiple mechanisms of IL6 signaling reinforcement involving myeloma cells and the hematologic microenvironment during extramedullary progression. Despite the prominent role of IL6 in myeloma progression, a clinical trial adding the anti-IL6 monoclonal antibody siltuximab to the bortezomib–melphalan–prednisone regimen did not improve the complete response rate or long-term outcome of transplant-ineligible patients with newly diagnosed multiple myeloma (50). Our study suggests this may be due to heterogeneity of the IL6 receptor expression among myeloma cells in those patients. For aggressive extramedullary myeloma, therapeutic strategies targeting multiple growth factors would be required to control pleiotropic growth stimulation.

In summary, we were able to demonstrate distinct gene-expression characteristics in refractory (relapsed) myeloma from pleural effusion or ascites consisting of pleiotropic auto- and paracrine-driven proliferation accompanied by the weakening of and evasion from the activated immune microenvironment. Analysis of intratumoral heterogeneity further demonstrated that preexisting myeloma cells had the potential for tumor progression and drug resistance. Our study has limitations of the small number of patients and zero-inflated gene-expression patterns in the single-cell RNA-seq data, in addition to the confounding factors for bone marrow versus extramedullary myeloma groups including the nature of microenvironment and the drug treatment for the extramedullary myeloma. Despite these limitations,

our comparative profiling of myeloma and the immune microenvironment revealed aspects and limitations of therapeutic interventions that could be used to design molecular therapeutic strategies for myeloma patients with aggressive extramedullary involvement.

#### Data availability

The scRNA sequencing and transcriptomic data in this paper have been submitted to the NCBI Gene-Expression Omnibus (GEO; <http://www.ncbi.nlm.nih.gov/geo/>) under accession numbers GSE106218 and GSE110499.

#### Disclosure of Potential Conflicts of Interest

No potential conflicts of interest were disclosed.

#### Authors' Contributions

**Conception and design:** H.-O. Lee, K. Kim, W.-Y. Park

**Acquisition of data (provided animals, acquired and managed patients, provided facilities, etc.):** S.J. Kim, H.-J. Kim, H.-O. Lee, K. Kim

**Analysis and interpretation of data (e.g., statistical analysis, biostatistics, computational analysis):** D. Ryu, S.J. Kim, Y. Hong, N. Kim, H.-J. Kim, H.-O. Lee, K. Kim, W.-Y. Park

**Writing, review, and/or revision of the manuscript:** D. Ryu, S.J. Kim, H.-O. Lee, K. Kim, W.-Y. Park

**Administrative, technical, or material support (i.e., reporting or organizing data, constructing databases):** A. Jo, K. Kim, W.-Y. Park

**Study supervision:** H.-O. Lee, K. Kim, W.-Y. Park

#### Acknowledgments

This work was supported by grants from the Ministry of Education (NRF-2017R1D1A1B03032194), the Ministry of Science and ICT (NRF-2016R1A5A1011974, NRF-2017M3A9A7050803, NRF-2017M3C9A6044636, and 2018M3C9A6017315), and the Ministry of Food and Drug Safety (16173MFDS004), Republic of Korea.

The costs of publication of this article were defrayed in part by the payment of page charges. This article must therefore be hereby marked *advertisement* in accordance with 18 U.S.C. Section 1734 solely to indicate this fact.

Received February 26, 2019; revised July 2, 2019; accepted September 23, 2019; published first September 26, 2019.

#### References

- Kuehl WM, Bergsagel PL. Molecular pathogenesis of multiple myeloma and its premalignant precursor. *J Clin Invest* 2012;122:3456–63.
- Madan S, Kumar S. Review: extramedullary disease in multiple myeloma. *Clin Adv Hematol Oncol* 2009;7:802–4.
- Braggio E, Kortum KM, Stewart AK. Snapshot: multiple myeloma. *Cancer Cell* 2015;28:678e1.
- Billecke L, Murga Penas EM, May AM, Engelhardt M, Nagler A, Leiba M, et al. Cytogenetics of extramedullary manifestations in multiple myeloma. *Br J Haematol* 2013;161:87–94.
- Decaux O, Lode L, Magrangeas F, Charbonnel C, Gouraud W, Jezequel P, et al. Prediction of survival in multiple myeloma based on gene expression profiles reveals cell cycle and chromosomal instability signatures in high-risk patients and hyperdiploid signatures in low-risk patients: a study of the Intergroupe Francophone du Myelome. *J Clin Oncol* 2008;26:4798–805.
- Manier S, Sacco A, Leleu X, Ghobrial IM, Roccaro AM. Bone marrow microenvironment in multiple myeloma progression. *J Biomed Biotechnol* 2012;2012:157496.
- Zheng GX, Terry JM, Belgrader P, Ryvkin P, Bent ZW, Wilson R, et al. Massively parallel digital transcriptional profiling of single cells. *Nat Commun* 2017;8:14049.
- Haber AL, Biton M, Rogel N, Herbst RH, Shekhar K, Smillie C, et al. A single-cell survey of the small intestinal epithelium. *Nature* 2017;551:333–9.
- Butler A, Hoffman P, Smibert P, Papalexi E, Satija R. Integrating single-cell transcriptomic data across different conditions, technologies, and species. *Nat Biotechnol* 2018;36:411–20.
- Aran D, Looney AP, Liu L, Wu E, Fong V, Hu A, et al. Reference-based analysis of lung single-cell sequencing reveals a transitional profibrotic macrophage. *Nat Immunol* 2019;20:163–72.
- Hanzelmann S, Castelo R, Guinney J. GSVA: gene set variation analysis for microarray and RNA-seq data. *BMC Bioinformatics* 2013;14:7.
- Subramanian A, Tamayo P, Mootha VK, Mukherjee S, Ebert BL, Gillette MA, et al. Gene set enrichment analysis: a knowledge-based approach for interpreting genome-wide expression profiles. *Proc Natl Acad Sci U S A* 2005;102:15545–50.
- Qiu X, Mao Q, Tang Y, Wang L, Chawla R, Pliner HA, et al. Reversed graph embedding resolves complex single-cell trajectories. *Nat Methods* 2017;14:979–82.
- Hay SB, Ferchen K, Chetal K, Grimes HL, Salomonis N. The Human Cell Atlas bone marrow single-cell interactive web portal. *Exp Hematol* 2018;68:51–61.

15. Bruns I, Cadeddu RP, Brueckmann I, Frobel J, Geyh S, Bust S, et al. Multiple myeloma-related deregulation of bone marrow-derived CD34(+) hematopoietic stem and progenitor cells. *Blood* 2012;120:2620–30.
16. Tirosh I, Izar B, Prakadan SM, Wadsworth MH, Treacy D II, Trombetta JJ, et al. Dissecting the multicellular ecosystem of metastatic melanoma by single-cell RNA-seq. *Science* 2016;352:189–96.
17. Miannay B, Minvielle S, Roux O, Drouin P, Avet-Loiseau H, Guerin-Charbonnel C, et al. Logic programming reveals alteration of key transcription factors in multiple myeloma. *Sci Rep* 2017;7:9257.
18. Tai YT, Acharya C, An G, Moschetta M, Zhong MY, Feng X, et al. APRIL and BCMA promote human multiple myeloma growth and immunosuppression in the bone marrow microenvironment. *Blood* 2016;127:3225–36.
19. Bergsagel PL, Kuehl WM, Zhan F, Sawyer J, Barlogie B, Shaughnessy J Jr. Cyclin D dysregulation: an early and unifying pathogenic event in multiple myeloma. *Blood* 2005;106:296–303.
20. Vallet S, Pozzi S, Patel K, Vaghela N, Fulciniti MT, Veiby P, et al. A novel role for CCL3 (MIP-1alpha) in myeloma-induced bone disease via osteocalcin downregulation and inhibition of osteoblast function. *Leukemia* 2011;25:1174–81.
21. Philp D, Scheremeta B, Sibliss K, Zhou M, Fine EL, Nguyen M, et al. Thymosin beta4 promotes matrix metalloproteinase expression during wound repair. *J Cell Physiol* 2006;208:195–200.
22. Lehnert C, Weiswange M, Jeremias I, Bayer C, Grunert M, Debatin KM, et al. TRAIL-receptor costimulation inhibits proximal TCR signaling and suppresses human T cell activation and proliferation. *J Immunol* 2014;193:4021–31.
23. Wu Y, Wang H. LncRNA NEAT1 promotes dexamethasone resistance in multiple myeloma by targeting miR-193a/MCL1 pathway. *J Biochem Mol Toxicol* 2018;32:e22008.
24. Dong G, Mao Q, Xia W, Xu Y, Wang J, Xu L, et al. PKM2 and cancer: the function of PKM2 beyond glycolysis. *Oncol Lett* 2016;11:1980–6.
25. Ledergor G, Weiner A, Zada M, Wang SY, Cohen YC, Gatt ME, et al. Single cell dissection of plasma cell heterogeneity in symptomatic and asymptomatic myeloma. *Nat Med* 2018;24:1867–76.
26. Keleg S, Kayed H, Jiang X, Penzel R, Giese T, Buchler MW, et al. Adrenomedullin is induced by hypoxia and enhances pancreatic cancer cell invasion. *Int J Cancer* 2007;121:21–32.
27. Lohr JG, Stojanov P, Carter SL, Cruz-Gordillo P, Lawrence MS, Auclair D, et al. Widespread genetic heterogeneity in multiple myeloma: implications for targeted therapy. *Cancer Cell* 2014;25:91–101.
28. Thiele B, Kloster M, Alawi M, Indenbirken D, Trepel M, Grundhoff A, et al. Next-generation sequencing of peripheral B-lineage cells pinpoints the circulating clonotypic cell pool in multiple myeloma. *Blood* 2014;123:3618–21.
29. Nutt SL, Hodgkin PD, Tarlinton DM, Corcoran LM. The generation of antibody-secreting plasma cells. *Nat Rev Immunol* 2015;15:160–71.
30. Lonial S, Durie B, Palumbo A, San-Miguel J. Monoclonal antibodies in the treatment of multiple myeloma: current status and future perspectives. *Leukemia* 2016;30:526–35.
31. Bacher R, Kendzierski C. Design and computational analysis of single-cell RNA-sequencing experiments. *Genome Biol* 2016;17:63.
32. Shi L, Campbell G, Jones WD, Campagne F, Wen Z, Walker SJ, et al. The MicroArray quality control (MAQC)-II study of common practices for the development and validation of microarray-based predictive models. *Nat Biotechnol* 2010;28:827–38.
33. Mulligan G, Mitsiades C, Bryant B, Zhan F, Chng WJ, Roels S, et al. Gene expression profiling and correlation with outcome in clinical trials of the proteasome inhibitor bortezomib. *Blood* 2007;109:3177–88.
34. Mahtouk K, Moreaux J, Hose D, Reme T, Meissner T, Jourdan M, et al. Growth factors in multiple myeloma: a comprehensive analysis of their expression in tumor cells and bone marrow environment using Affymetrix microarrays. *BMC Cancer* 2010;10:198.
35. Sanz-Rodriguez F, Teixido J. VLA-4-dependent myeloma cell adhesion. *Leuk Lymphoma* 2001;41:239–45.
36. Meads MB, Fang B, Mathews L, Gemmer J, Nong L, Rosado-Lopez I, et al. Targeting PYK2 mediates microenvironment-specific cell death in multiple myeloma. *Oncogene* 2016;35:2723–34.
37. Shiozawa Y, Havens AM, Pienta KJ, Taichman RS. The bone marrow niche: habitat to hematopoietic and mesenchymal stem cells, and unwitting host to molecular parasites. *Leukemia* 2008;22:941–50.
38. Carbone E, Neri P, Mesuraca M, Fulciniti MT, Otsuki T, Pende D, et al. HLA class I, NKG2D, and natural cytotoxicity receptors regulate multiple myeloma cell recognition by natural killer cells. *Blood* 2005;105:251–8.
39. Carbone E, Terrazzano G, Melian A, Zanzi D, Moretta L, Porcelli S, et al. Inhibition of human NK cell-mediated killing by CD1 molecules. *J Immunol* 2000;164:6130–7.
40. Garrido F, Ruiz-Cabello F, Cabrera T, Perez-Villar JJ, Lopez-Botet M, Duggan-Keen M, et al. Implications for immunosurveillance of altered HLA class I phenotypes in human tumours. *Immunol Today* 1997;18:89–95.
41. Zhang Y, Lu N, Xue Y, Zhang M, Li Y, Si Y, et al. Expression of immunoglobulin-like transcript (ILT)2 and ILT3 in human gastric cancer and its clinical significance. *Mol Med Rep* 2012;5:910–6.
42. Kang X, Kim J, Deng M, John S, Chen H, Wu G, et al. Inhibitory leukocyte immunoglobulin-like receptors: immune checkpoint proteins and tumor sustaining factors. *Cell Cycle* 2016;15:25–40.
43. Barsoum IB, Smallwood CA, Siemens DR, Graham CH. A mechanism of hypoxia-mediated escape from adaptive immunity in cancer cells. *Cancer Res* 2014;74:665–74.
44. Oerlemans R, Franke NE, Assaraf YG, Cloos J, van Zantwijk I, Berkers CR, et al. Molecular basis of bortezomib resistance: proteasome subunit beta5 (PSMB5) gene mutation and overexpression of PSMB5 protein. *Blood* 2008;112:2489–99.
45. Hose D, Reme T, Hielscher T, Moreaux J, Messner T, Seckinger A, et al. Proliferation is a central independent prognostic factor and target for personalized and risk-adapted treatment in multiple myeloma. *Haematologica* 2011;96:87–95.
46. Mitra AK, Mukherjee UK, Harding T, Jang JS, Stessman H, Li Y, et al. Single-cell analysis of targeted transcriptome predicts drug sensitivity of single cells within human myeloma tumors. *Leukemia* 2016;30:1094–102.
47. Pittari G, Vago L, Festuccia M, Bonini C, Mudawi D, Giaccone L, et al. Restoring natural killer cell immunity against multiple myeloma in the era of new drugs. *Front Immunol* 2017;8:1444.
48. Burger R. Impact of interleukin-6 in hematological malignancies. *Transfus Med Hemother* 2013;40:336–43.
49. Shain KH, Yarde DN, Meads MB, Huang M, Jove R, Hazlehurst LA, et al. Beta1 integrin adhesion enhances IL-6-mediated STAT3 signaling in myeloma cells: implications for microenvironment influence on tumor survival and proliferation. *Cancer Res* 2009;69:1009–15.
50. San-Miguel J, Blade J, Shpilberg O, Grosicki S, Maloel F, Min CK, et al. Phase 2 randomized study of bortezomib-melphalan-prednisone with or without siltuximab (anti-IL-6) in multiple myeloma. *Blood* 2014;123:4136–42.